

## SELF-ADAPTIVE COMPENSATION METHOD OF THERMAL ERROR FOR HOBGING MACHINE TOOL

SHUAI YANG<sup>1,\*</sup>, XING LUO<sup>2</sup>, XU CHEN<sup>2</sup> AND ZHIYONG LUO<sup>3</sup>

<sup>1</sup>National Research Base of Intelligent Manufacturing Service

<sup>2</sup>School of Management Science and Engineering

Chongqing Technology and Business University

No. 19, Xuefu Avenue, Nan'an District, Chongqing 400067, P. R. China

\*Corresponding author: jerryyang@ctbu.edu.cn; { luoxing0120; chenxu2755473272 }@163.com

<sup>3</sup>Chongqing Banan District Quality Monitor Center of Road Engineering

No. 2-20, Longzhou Avenue, Banan District, Chongqing 401320, P. R. China

617548164@qq.com

Received April 2021; revised August 2021

**ABSTRACT.** *For the gear hobbing machine tool, the manufacturing precision of gears is usually reduced by the thermal deformation from the main spindles. To minimize this thermal error, a self-adaptive compensation method is proposed in this paper. The optimal temperature measuring points are determined by the weighted grey correlativity at the initial stage. With the data from temperature and displacement sensors, the mathematical model of thermal error compensation is established through the least-square method. The self-adaptive compensation program is developed based on siemens numerical control (NC) system. The experiments are carried out to verify the accuracy of this self-adaptive compensation method, and the results show that the overall improvement of gear thermal error reaches 11.75%.*

**Keywords:** Self-adaptive compensation, Thermal errors, Hobbing machine, Weighted grey correlativity, NC system

**1. Introduction.** For the gear manufacturing industry, vibration and thermal error of machine tool are two significant factors related to gear precision, which can cause as high as 80% of the whole machine error [1-3]. Especially for gear hobbing machine, the thermal error can lead to a severe reduction of gear precision. Thermal error is usually caused by two major sources, external and internal, respectively [4-6]. For external source, it represents the environmental temperature of machine tool. To limit this effect, many companies choose to build constant temperature factories. As another source, the internal source is generated by friction, cutting process and movement of machine tool, which contribute the major thermal error during the gear manufacturing [7-10].

In the last several decades, to minimize the effect caused by thermal error, many researchers have been conducting comparative researches, and much progress has been archived. Most of the proposed methods can be classified into two types [11-13]. By using a cooling system for machine tool, the thermal errors can be limited to a low level, which is the first type. Dubrov proposed a self-contained two-phase cooling system, and the experiments show promising results for machine cooling [14]. However, more attention is drawn to the second type, which is thermal errors compensation. By revealing the relationship between the deformation and temperature of the machine tool, the compensation model can be built [15-17].

Reddy et al. proposed a real-time compensation method for thermal error by using feed-forward backpropagation neural network regression analysis technique, algorithm development. Experiments were carried out to verify the effectiveness of the method [18]. Through Python programming language, Mareš et al. used transfer functions to build the mathematical model and directly implemented it into the control system of a gear milling machine. Results show the precision of gear has been improved [19]. Li et al. built an explicit error model for heavy machine tool, which was verified by the simulation FEM (finite element modeling) [20].

As mentioned above, much progress has been achieved for the thermal error compensation of machine tool during the last two decades. However, most previous works are prone to installing extra thermal compensation devices or redesigning the whole machine tool with their thermal error models. These solutions will increase the cost and reduce the reliability of the machine tool at the same time. Moreover, a new installment or redesign of a machine tool requires tremendous experimental verification, which leads to a more prolonged product development stage. In this work, a self-adaptive compensation method of thermal error embedded in the siemens numerical control (NC) system is proposed. With several temperature sensors, the proposed method can achieve real-time error compensation during the hobbing process of gear through the NC system.

**2. Problem Statement and Preliminaries.** As it is shown in Figure 1, the researching subject is a double spindle vertical NC gear hobbing machine.  $a$  is the diameter of the main spindle,  $b$  is the diameter of the small spindle,  $x$  is the distance between the center of the main spindle and the center of the hobbing cutter,  $X_0$  is the distance between the center of the hobbing cutter and the center of rotation platform, and  $L$  is the distance between the center of two spindles.  $H_1$  is the height of the main spindle,  $H_2$  is the height of the small spindle,  $H_3$  is the distance between the center of the hobbing cutter and the rotation platform, and  $H$  is the height of the rotation platform. Due to its complicated structure, more temperature sensors are required to build an accurate thermal error model. However, more sensors will also lead to more problems. 1) The limitation of physical space. Due to the complicated working environment and structure, the actual physical space for

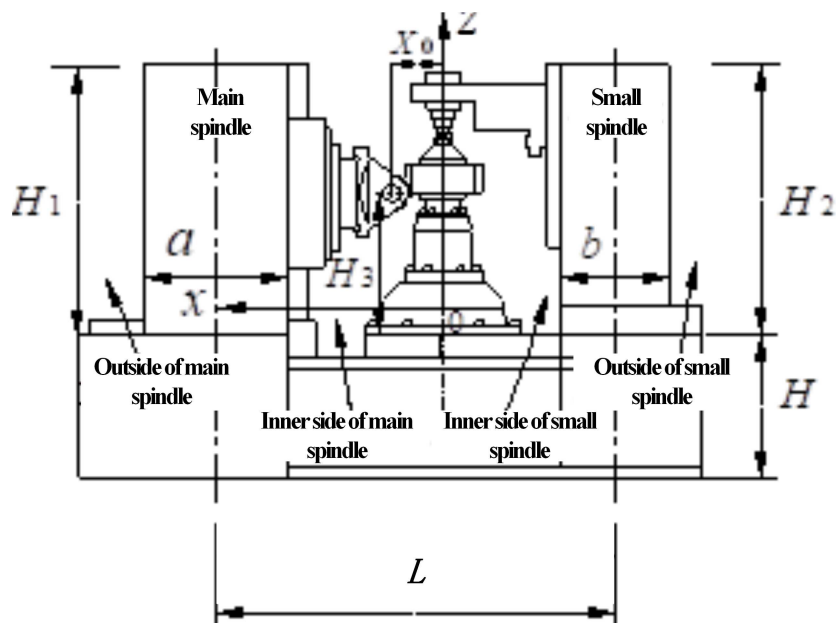


FIGURE 1. The structural diagram of the NC gear machine tool

temperature sensors is limited. 2) Data redundancy. With more sensors, there will be tremendous redundant data, which will lower the efficiency of the NC system and affect the accuracy of the compensation model.

To solve the above problems, the placement of temperature measuring points has to be optimized. The weighted grey correlativity is applied to analyzing the primary source of thermal error in this paper, which can determine the optimal measuring locations for temperature sensors with small data sets.

**2.1. The placement of initial measuring points.** According to the thermal deformation of the double spindles vertical NC gear hobbing machine, 16 locations are chosen as the initial temperature measuring points ( $T_1$ - $T_{16}$ ), which are shown in Figure 2. Two displacement sensors ( $X_1$  and  $X_2$ ) are located at the hobbing shaft and holder shaft of gear. With the data from temperature and displacement sensors, the relationship between the deformation of two spindles and temperature can be revealed, which leads to the optimization for the location of temperature sensors.

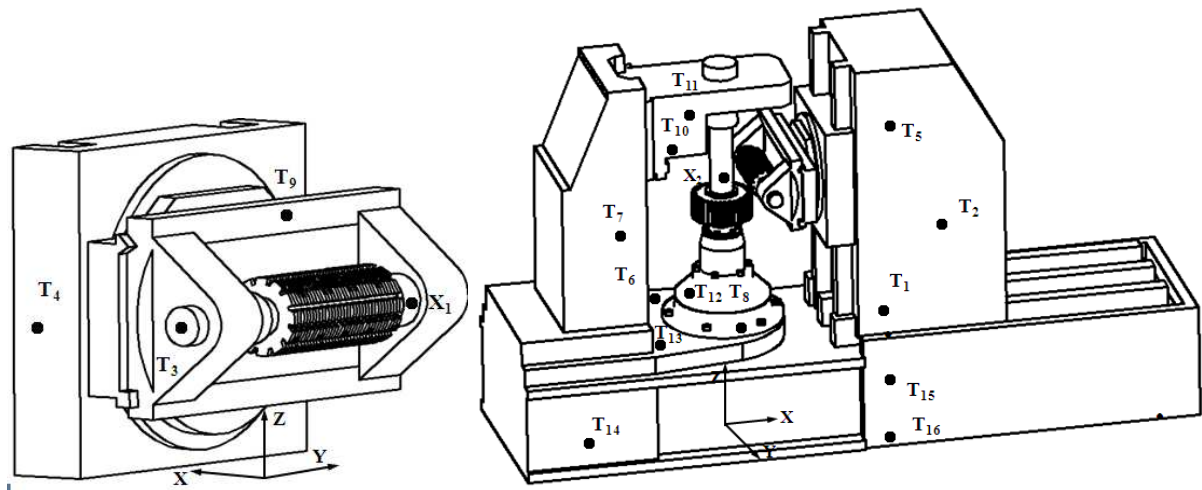


FIGURE 2. The placement of initial measuring points

**2.2. The selection of temperature measuring points.** Under the actual working condition, it always takes a long period to reach the stable temperature for the gear hobbing machine tool, and the ascending curve of temperature also shows a steady trending. Therefore, the sampling frequency in this type of experiment can be set at a low level. In this paper, the sampling interval is 0.5 minute, and the time span is from the beginning of the gear hobbing process to the temperature of the machine tool reaches stable. The part of the experimental data is shown in Figure 3.  $T_1$ - $T_{16}$  are temperatures from sensors  $T_1$ - $T_{16}$ ,  $S_1$  and  $S_2$  stand for the displacements from sensors  $X_1$  and  $X_2$ .

As it is mentioned before, the data from temperature and displacement sensors are small data sets. To archive a higher accurate result, the weighted grey relational analysis model is applied to choosing the optimal location for temperature sensors.  $X = \{x_\sigma | \sigma = 0, 1, \dots, 17\}$  is defined as the sequence association of subsets, the thermal deformation  $x_0$  of the hobbing shaft ( $X_1$ ) and  $x_{17}$  of the holder shaft ( $X_2$ ) are the dominant factors,  $x_i$  is the sub-factor ( $i = 1, 2, \dots, 16$ ),  $x_\sigma(k)$  represents the value of  $x_\sigma$  in  $k$  point. Data are divided into 6 groups, where  $k = 1, 2, \dots, 90$ .  $x'(k)$  is assumed as the accumulative subtraction for generating sequence  $x(k)$  of  $x'(k) = x(k) - x(k-1)$ , ( $k = 1, 2, \dots, 90$ ).

Time	T <sub>1</sub>	T <sub>2</sub>	T <sub>3</sub>	T <sub>4</sub>	T <sub>5</sub>	T <sub>6</sub>	T <sub>7</sub>	T <sub>8</sub>	T <sub>9</sub>	T <sub>10</sub>	T <sub>11</sub>	T <sub>12</sub>	T <sub>13</sub>	T <sub>14</sub>	T <sub>15</sub>	T <sub>16</sub>	S <sub>1</sub>	S <sub>2</sub>
9:03:00	11.64	12.39	12.11	15.24	13.85	11.31	11.09	11.45	14.29	11.68	11.72	11.09	10.93	11.05	11.2481	11.5352	0	0
9:03:28	11.64	12.26	12.11	15.19	13.78	11.43	11.06	11.43	14.27	11.72	11.81	11.09	10.93	11.02	11.23	11.54	-0.0001	0.0233
9:03:56	11.60	12.20	12.06	15.13	13.74	11.31	10.97	11.45	14.27	11.70	11.76	10.97	10.84	10.94	11.25	11.50	-0.0015	0.0136
9:04:28	11.56	12.24	12.24	15.19	13.77	11.53	11.06	11.78	14.45	11.68	11.81	11.09	11.03	11.00	11.57	11.46	-0.0026	0.0317
9:04:56	11.76	12.39	12.43	15.21	14.03	11.39	11.09	11.99	14.60	11.70	11.76	11.03	10.89	11.02	11.78	11.65	-0.005	0.0802
9:05:28	12.56	12.56	12.49	15.24	13.95	11.51	11.01	12.28	16.44	11.86	11.99	11.14	11.01	10.97	12.06	12.45	-0.0043	0.0287
9:05:56	12.87	12.68	12.56	15.30	13.95	11.61	11.20	12.01	16.58	11.86	11.99	11.11	11.14	11.14	11.80	12.75	-2.1121	5.2889
9:06:28	12.31	12.56	12.45	15.24	13.99	11.51	11.01	11.85	16.27	11.86	11.86	11.14	11.06	10.95	11.64	12.20	-0.003	0.0757
9:06:56	12.26	12.62	12.45	15.30	14.07	11.60	11.09	12.10	16.08	11.89	11.99	11.09	11.03	11.02	11.89	12.15	-0.0037	0.0219
9:07:28	12.26	12.56	12.43	15.21	14.03	11.60	11.09	12.20	16.15	11.89	11.95	11.20	11.18	11.02	11.98	12.15	-0.0054	0.0925
9:07:56	12.49	12.62	12.64	15.52	14.35	11.51	11.09	12.43	17.40	11.89	12.06	11.20	11.18	11.06	12.21	12.38	-0.0055	0.0205
9:08:28	13.52	12.76	12.49	15.52	14.37	11.60	11.18	12.31	17.67	11.86	12.10	11.09	11.06	11.17	12.09	13.40	-2.1122	5.2263
9:08:56	13.10	12.64	12.49	15.55	14.45	11.53	11.11	12.11	17.33	11.81	12.10	11.11	11.14	11.06	11.90	12.98	-2.1122	5.2705
9:09:28	12.68	12.53	12.37	15.71	14.49	11.60	11.11	12.01	17.02	12.01	12.18	11.14	11.18	11.08	11.80	12.57	0.0008	0.0683
9:09:56	12.68	12.56	12.45	15.71	14.54	11.53	11.20	12.11	16.90	12.01	12.18	11.22	11.18	11.15	11.90	12.57	-0.0022	0.0274
9:10:28	13.52	12.64	12.49	15.83	14.54	11.51	11.11	13.35	17.00	11.93	12.18	11.22	11.26	11.05	13.11	13.40	-0.0067	0.0591
9:10:56	13.39	12.78	12.56	16.02	14.69	11.51	11.06	13.03	17.54	11.89	12.35	11.11	11.18	11.02	12.80	13.27	-0.0063	0.1119
9:11:28	13.02	12.93	12.49	16.08	14.70	11.60	11.11	12.70	17.63	11.93	12.37	11.20	11.18	11.09	12.48	12.90	-2.1124	5.2701
9:11:56	12.93	12.85	12.53	16.13	14.79	11.61	11.11	12.62	17.52	12.03	12.37	11.20	11.26	11.05	12.40	12.81	-0.0027	0.1025
9:12:28	12.56	12.68	12.45	16.27	14.85	11.61	11.18	12.28	17.38	11.99	12.26	11.20	11.22	11.15	12.06	12.45	-0.0029	0.0965
9:12:56	12.74	12.74	12.53	16.44	14.95	11.64	11.11	12.53	17.81	11.99	12.26	11.22	11.26	11.10	12.31	12.63	-0.0039	0.0956
9:13:28	13.95	12.85	12.64	16.69	15.16	11.72	11.11	12.70	18.36	12.01	12.35	11.20	11.22	11.09	12.48	13.82	-0.004	0.0618
9:13:56	13.95	12.74	12.62	16.77	15.20	11.78	11.11	12.53	18.47	12.03	12.28	11.26	11.28	11.07	12.31	13.82	-2.1126	5.3007
9:14:28	13.39	12.76	12.56	17.00	15.33	11.89	11.18	12.39	18.22	12.03	12.24	11.22	11.28	11.13	12.17	13.27	-0.0025	0.0636
9:14:56	12.99	12.64	12.49	17.00	15.37	11.70	11.11	12.28	18.06	11.99	12.18	11.20	11.22	11.04	12.06	12.87	-0.0033	0.0472
9:15:28	12.70	12.62	12.56	17.19	15.33	11.78	11.18	12.31	18.09	12.01	12.24	11.20	11.26	11.13	12.09	12.59	-0.0046	0.0635

FIGURE 3. The part of the experimental data

For  $x_0$  and  $x_i$

$$\left\{ \begin{aligned} \zeta_i(k) &= \frac{\xi \cdot \max_{i \in 16} \max_{k \in 90} |x_0(k) - x_i(k)|}{\lambda_1 \left| x_0(k) - x_i(k) \right| + \lambda_2 \left| x'_0(k) - x'_i(k) \right| + \xi \cdot \max_{i \in 16} \max_{k \in 90} |x_0(k) - x_i(k)|} \\ \gamma_i &= \gamma(x_0, x_i) = \frac{1}{90} \cdot \sum_{k=1}^{90} \zeta_i(k) \end{aligned} \right. \quad (1)$$

In Equation (1) the distinguishing coefficient  $\xi$  is 0.5, displacement weighted coefficient and changing rate weighted coefficient are also chosen as 0.5 [14,17,21].  $\gamma_i$  is grey correlativity between  $x_i$  and  $x_0$ , and  $\gamma'_i$  is grey correlativity between  $x_i$  and  $x_{17}$ .

By inputting all the data into Equation (1), through the software Matlab, the grey correlativity between  $x_i$  and  $x_0$  can be determined as:

$$\begin{aligned} \gamma_1 &= 0.711 & \gamma_2 &= 0.692 & \gamma_3 &= 0.866 & \gamma_4 &= 0.811 & \gamma_5 &= 0.591 & \gamma_6 &= 0.718 \\ \gamma_7 &= 0.717 & \gamma_8 &= 0.647 & \gamma_9 &= 0.803 & \gamma_{10} &= 0.764 & \gamma_{11} &= 0.652 & \gamma_{12} &= 0.838 \\ \gamma_{13} &= 0.755 & \gamma_{14} &= 0.792 & \gamma_{15} &= 0.579 & \gamma_{16} &= 0.467 \end{aligned}$$

According to the results, the six biggest grey correlativity are  $\gamma_3, \gamma_{12}, \gamma_4, \gamma_9, \gamma_{14}, \gamma_{10}$  respectively. Through the same process, the grey correlativity of  $\gamma'_i$  can also be calculated, which are  $\gamma'_7, \gamma'_{10}, \gamma'_4, \gamma'_{13}, \gamma'_{12}, \gamma'_3$  respectively. By comparing the two groups of grey correlativity, points 3, 4, 10 and 12 exist in both groups. Therefore, placement points of  $T_3, T_4, T_{10}$  and  $T_{12}$  are chosen as the optimal temperature measuring points to build the compensation model.

**3. The Compensation Model of Thermal Error.** In the former section, four optimal temperature measuring points were selected as the data resource to construct the compensation model for the gear hobbing machine. The experimental test rigs are shown in Figure 4.

The least-square method is employed to build the thermal error compensation model, which can not only generate the fitting equation efficiently, but also provide a high precision [22]. The relationship between displacements and temperatures can be demonstrated

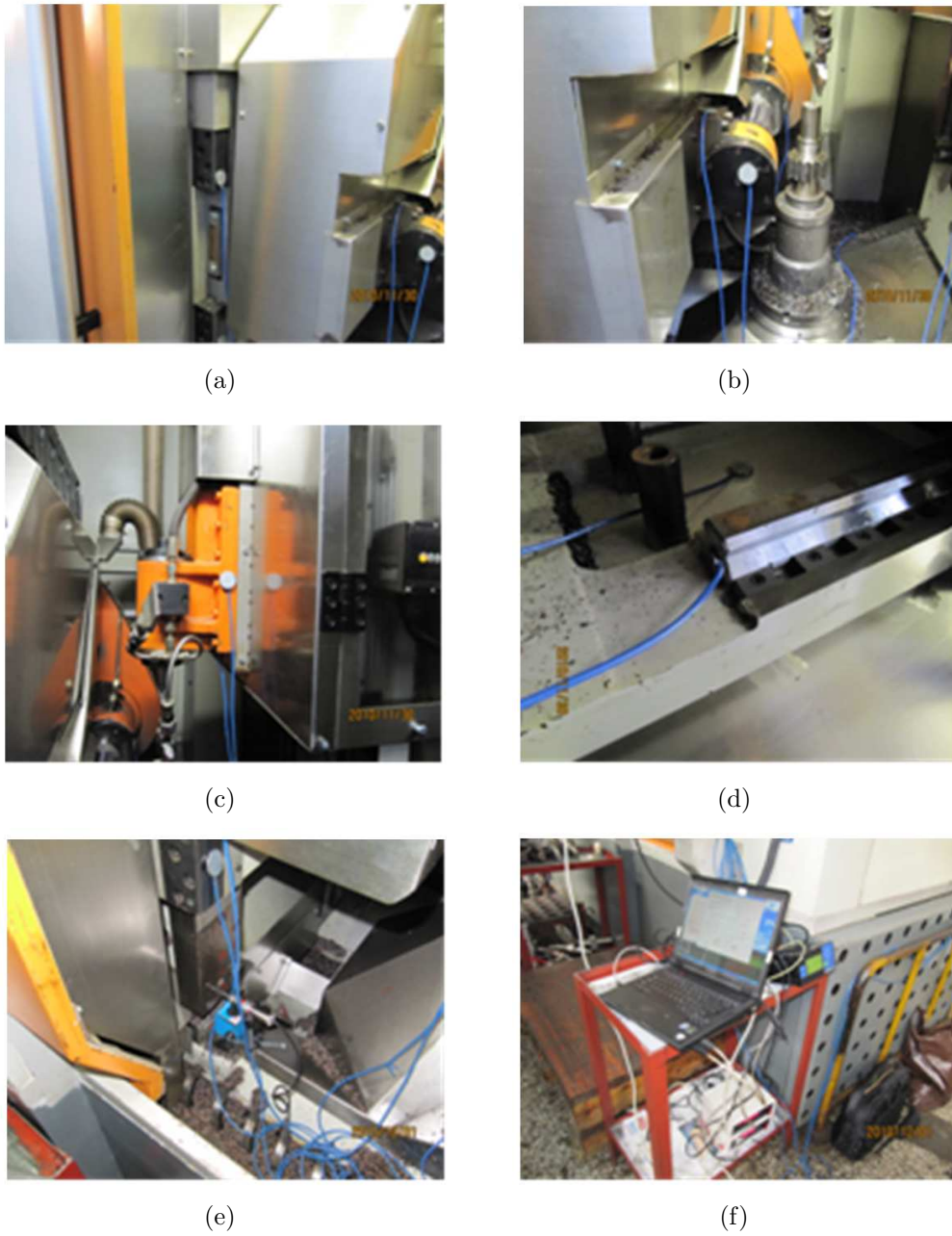


FIGURE 4. The experimental test rigs. (a), (b), (c), (d) are the placement of temperature sensors  $T_3$ ,  $T_4$ ,  $T_{10}$  and  $T_{12}$  respectively, (e) is the placement of displacement sensors  $X_1$  and  $X_2$ , and (f) is the data acquisition system.

by the matrix equation, which is

$$\begin{pmatrix} 1 & t_{11} & \cdots & t_{1m} \\ 1 & t_{21} & \cdots & t_{2m} \\ \vdots & \vdots & \cdots & \vdots \\ 1 & t_{n1} & \cdots & t_{nm} \end{pmatrix} \begin{pmatrix} a_0 \\ a_1 \\ \vdots \\ a_m \end{pmatrix} + \begin{pmatrix} \varepsilon_1 \\ \varepsilon_2 \\ \vdots \\ \varepsilon_n \end{pmatrix} = \begin{pmatrix} y_1 \\ y_2 \\ \vdots \\ y_n \end{pmatrix} \quad (2)$$

In this equation,  $t_{ij}$  stands for the temperature from the optimal measuring point ( $m$  represents the number of sensors, and  $n$  is the number of data units),  $a_i$  represents the undetermined coefficient, and  $y_j$  is defined as the deformation corresponding to the temperature.

With the least-square method, the equation can be rewritten as:

$$\begin{cases} \min(\varepsilon_1)^2 = (y_1 - a_0 - a_1t_{11} - \dots - a_mt_{1m})^2 \\ \min(\varepsilon_2)^2 = (y_2 - a_0 - a_1t_{21} - \dots - a_mt_{2m})^2 \\ \vdots \\ \min(\varepsilon_n)^2 = (y_n - a_0 - a_1t_{n1} - \dots - a_mt_{nm})^2 \end{cases} \tag{3}$$

In Equation (3), the  $\varepsilon_i$  is the compensation displacement. Since the minimal value of  $(\varepsilon_i)^2$  exists, it can be calculated by the following equation:

$$-2 \sum_{j=0}^n \left[ y_j - \sum_{i=0}^m a_i \varphi_i(t_{ij}) \right] \varphi_k(t_{ij}) = 0, \quad (k = 0, 1, 2, \dots, m) \tag{4}$$

Then the equation group can also be determined by

$$\left. \begin{aligned} -2 \sum_{j=1}^n (y_j - a_0 - a_1t_{j1} - a_2t_{j2} - \dots - a_mt_{jm}) &= 0 \\ -2 \sum_{j=1}^n (y_j - a_0 - a_1t_{j1} - a_2t_{j2} - \dots - a_mt_{jm}) t_{j1} &= 0 \\ &\vdots \\ -2 \sum_{j=1}^n (y_j - a_0 - a_1t_{j1} - a_2t_{j2} - \dots - a_mt_{jm}) t_{jm} &= 0 \end{aligned} \right\} \tag{5}$$

By substituting the data from temperature and displacement sensors into Equation (5), the key coefficients  $a_0, a_3, a_4, a_{12}$  can be calculated, which are  $-0.2565, 0.0189, -0.0124, 0.0082, -0.0074$  respectively. The thermal error compensation model of main spindle in the horizontal direction can be written as:

$$x_m = -0.2565 + 0.0189T_3 - 0.0124T_4 + 0.0082T_{10} - 0.0074T_{12} \tag{6}$$

Through the same procedure, the thermal error compensation model of small spindle in the horizontal direction can also be determined as:

$$x_s = -0.1493 - 6.2945T_4 + 7.7619T_8 - 4.0562T_{10} + 4.1436T_{12} \tag{7}$$

#### 4. Self-Adaptive Compensation Based on Siemens NC System.

**4.1. The construction of the program for self-adaptive compensation.** To satisfy the individuality demand, more companies launch the open numerical control system, which can be second-developed by customers. In this research, the Siemens NC system is chosen due to its characteristics of open source. With coding software like Visual Basic and Visual C, the function of the NC system can be various under Siemens HMI Package [23]. Based on these software packages, the self-adaptive compensation program is developed. The flow chart of this program is shown in Figure 5. The working sequence for this program is listed as the following.

Step 1: Programmable logic controller (PLC) receives all the data from temperature and displacement sensors.

Step 2: Program accesses PLC and convert all the data into a text file.

Step 3: NC system accesses the text file and decides to re-build the mathematical model or not.

Step 4: Access the temperature value of PLC to calculate the compensation value.

Step 5: Endow the results to R parameters.

Step 6: Transmit the R parameter to NCK.

Step 7: Generate the G code for the NC gear hobbing machine.

Based on Figure 5, the compensation model of this program is consistently re-built according to different situations. When the relationship between temperature and deformation changes, such as the working environment, and the re-installation of the machine tool, this program will automatically modify the compensation model to maintain the accuracy.

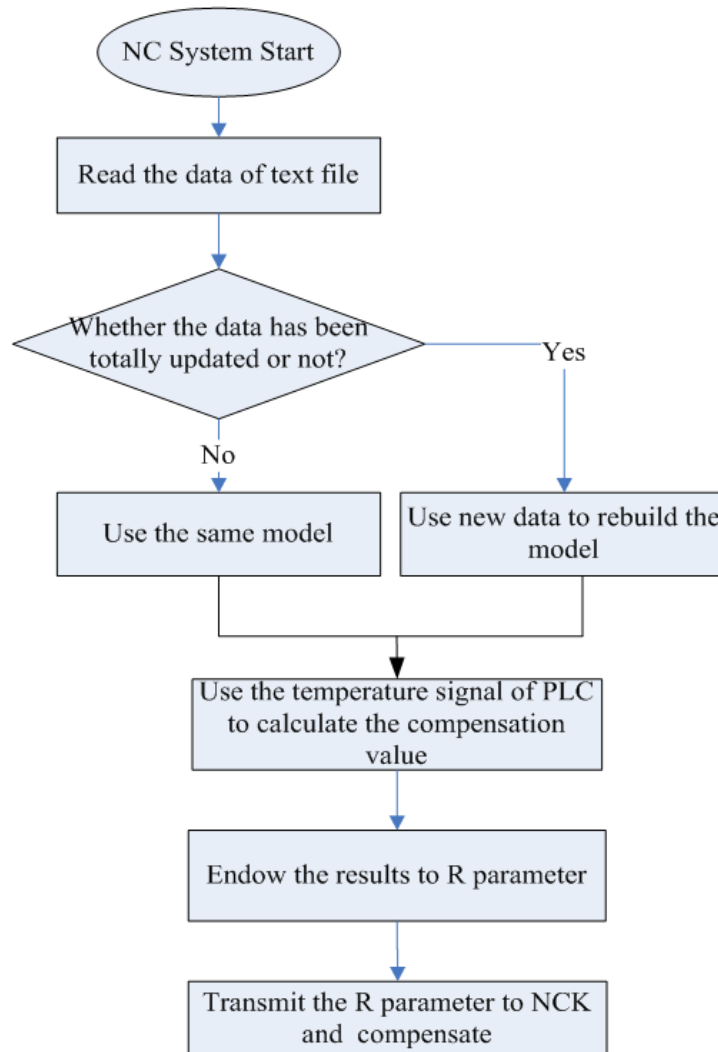


FIGURE 5. The flow chart of the adaptive compensation program

**4.2. The construction of hardware for self-adaptive compensation.** Since most NC systems are installed on computers of the machine tool, the self-adaptive compensation program can be embedded into the NC system directly due to its computing capacity. With PLC, digital-analog (D/A) converter, temperature and displacement sensors, which is built by the following steps.

Step 1: Selection of suitable temperature and displacement sensors. In this paper, Pt-1000 thermal sensor and TG105 grating displacement sensor are chosen, due to their low costs and high reliability.

Step 2: Selection of D/A converter. Since the temperature sensors can only generate analog signals, AD9171 D/A converter is selected to convert the data for PLC.

Step 3: Selection of PLC (Siemens S7-200).

Step 4: Distribution of the temperature and displacement sensors on the machine tool.

Step 5: Connect the sensors, D/A converter, PLC and NC system, and make sure the data transmission is successful.

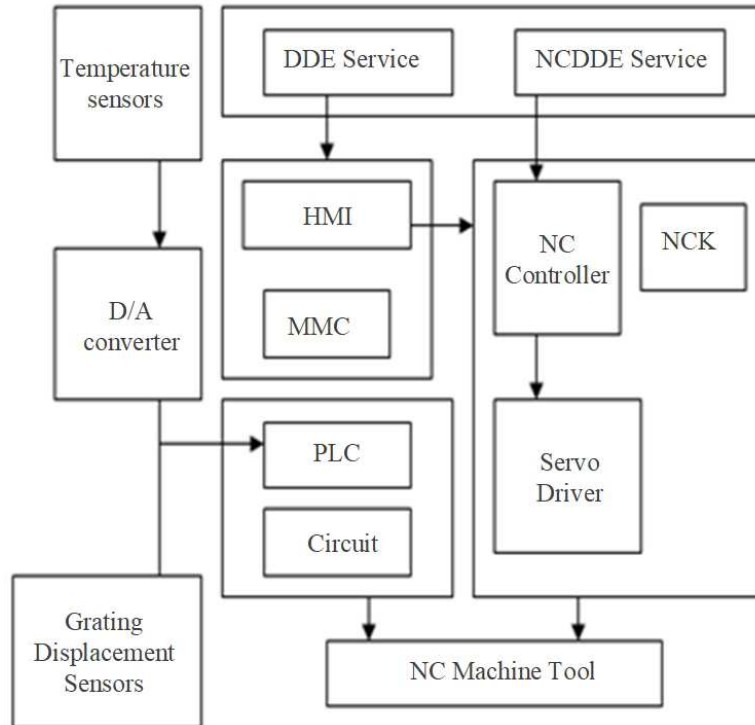


FIGURE 6. The construction diagram of the hardware for self-adaptive compensation

The construction diagram of the hardware is shown in Figure 6. After the start of the NC system, the data from temperature and displacement sensors will be transferred to PLC through a D/A converter, which will be stored in the NC system as a text file. The proposed self-compensation program will access this file and build the mathematical model. With the real-time data from temperature sensors, this program can generate the G codes with compensation value and transmit them to the NC system, which eventually leads to the achievement of self-adaptive thermal compensation for gear hobbing NC machine tool. The specific parameters for hardware devices are listed in Table 1.

**5. Experimental Verification.** To verify the efficiency of this compensation method, the same NC gear hobbing machine tool manufactures every 1000 pieces of gear with and without a self-adaptive compensation program. Two batches of gears are compared in tooth profile error, tooth alignment error, geometric eccentricity error and eccentric motion error respectively. The results are shown in Table 2.

Based on Table 2, the gear hobbing NC machine tool with a self-adaptive compensation program shows improvement in all four errors of gear manufacturing, the overall improvement of precision is 11.75%, which indicates the efficiency of the proposed compensation method.

**6. Conclusions.** In this paper, a self-adaptive compensation method is proposed for the NC gear hobbing machine. To avoid data redundancy, the weighted grey correlativity is applied to choosing the optimal temperature measuring points. With the data from

TABLE 1. The specific parameters of hardware devices

Item	Model	Specific parameters
Thermal sensor	Pt-1000	Working current, $\leq 0.3$ mA Insulation resistance, $\geq 100$ M $\Omega$ (100 V DC) Endurance voltage, 3000 V AC (60 S) Working temperature, $-50^{\circ}\text{C} \sim 200^{\circ}\text{C}$ Flame retardant rating, UL94V-0 Protection grade, IP67
Grating displacement sensor	TG105	Measuring range, 0 mm $\sim$ 15 mm Resolution, 0.001 mm Output signal, 5 V TTL square wave Working temperature, $0^{\circ}\text{C} \sim 50^{\circ}\text{C}$
D/A converter	AD9171	Resolution, 16 Bits Full-Scale Output Current, 14.2 mA $\sim$ 28.8 mA Working temperature, $-40^{\circ}\text{C} \sim 118^{\circ}\text{C}$ Data channel, 6
PLC	Siemens S7-200	Working voltage, DC 24 V, AC 100 $\sim$ 230 V, Working temperature, $-0^{\circ}\text{C} \sim 55^{\circ}\text{C}$ Program memory, 8K Bits Data memory, 2.5K Bits Protection grade, IP20 $\sim$ IEC529

TABLE 2. The improvement ratio with self-adaptive compensation method

Number	Error type	Improvement ratio
1	Tooth profile error	17%
2	Tooth alignment error	12%
3	Geometric eccentricity error	7%
4	Eccentric motion error	11%
Overall		11.75%

all the sensors, the mathematical model of thermal compensation is established by the least-square method, which demonstrates the relationship between temperature and compensation displacement. The compensation program structure is developed under the Siemens NC system, which can generate G codes with real-time temperature data, which can generate G codes with real-time temperature data. Two batches of gears are chosen for the comparison, and results show the overall improvement of gear precision is 11.75% with the proposed compensation method. In our future work, thermal camera will be employed instead of temperature sensor. With image identification algorithm, key deformation points can be easily located. Furthermore, comparisons with other compensation methods will be carried out to verify the efficiency of the proposed method.

**Acknowledgment.** This research is supported by National Natural Science Foundation of China (51905058), Natural Science Foundation of Chongqing (cstc2020jcyj-msxmX0182), Science and Technology Research Program of Chongqing Municipal Education Commission (KJQN201800830), Research Start-Up Funds of Chongqing Technology and Business University (1856018), Key Research Platform Project of Chongqing Technology and Business University (ZDPTTD201918). The authors also gratefully acknowledge the helpful comments and suggestions of the reviewers, which have improved the presentation.

## REFERENCES

- [1] Y. Kang, C. W. Chang, Y. R. Huang, C. L. Hsu and I-F. Nieh, Modification of a neural network utilizing hybrid filters for the compensation of thermal deformation in machine tools, *International Journal of Machine Tools and Manufacture*, vol.47, pp.376-387, 2006.
- [2] M. A. Donmez, M. H. Hahn and J. A. Soons, A novel cooling system to reduce thermally-induced errors of machine tools, *Annals of the CIRP*, vol.56, pp.521-524, 2007.
- [3] H. Wu, H. T. Zhang, Q. J. Guo, X. S. Wang and J. G. Yang, Thermal error optimization modeling and real-time compensation on a CNC turning center, *Journal of Materials Processing Technology*, vol.207, pp.172-179, 2008.
- [4] Y. Li, W. H. Zhao, S. H. Lan, J. Ni, W. W. Wu and B. H. Lu, A review on spindle thermal error compensation in machine tools, *International Journal of Machine Tools and Manufacture*, vol.95, pp.20-38, 2015.
- [5] M. Fujishima, K. Narimatsu, N. Irino, M. Mori and S. Ibaraki, Adaptive thermal displacement compensation method based on deep learning, *CIRP J. Manu. of Sci. Technol.*, vol.25, pp.22-25, 2019.
- [6] X. Yao, T. Hu, G. Yin and C. Cheng, Thermal error modeling and prediction analysis based on OM algorithm for machine tool's spindle, *Int. J. Adv. Manu. of Technol.*, vol.106, pp.3345-3356, 2020.
- [7] L. Chen, G. Xu, S. Zhang, W. Yan and Q. Wu, Health indicator construction of machinery based on end-to-end trainable convolution recurrent neural networks, *J. Manu. of Syst.*, vol.54, pp.1-11, 2020.
- [8] F. Li, T. Li, H. Wang and Y. Jiang, A temperature sensor clustering method for thermal error modelling of heavy milling machine tools, *Appl. Sci.*, vol.7, no.1, pp.82-93, 2017.
- [9] C. Ma, L. Zhao, X. Mei, H. Shi and J. Yang, Thermal error compensation of high-speed spindle system based on a modified BP neural network, *Int. J. Adv. Manu. of Technol.*, vol.89, pp.3071-3085, 2016.
- [10] R.-C. Wu, C.-L. Pan and C.-Y. Chen, Parameter estimation for permanent magnet DC machine by least square method, *ICIC Express Letters*, vol.11, no.10, pp.1571-1578, 2017.
- [11] J. L. Liu, C. Ma and S. L. Wang, Data-driven thermally-induced error compensation method of high-speed and precision five-axis machine tools, *Mechanical Systems and Signal Processing*, vol.138, DOI: 10.1016/j.ymssp.2019.106538, 2020.
- [12] M. Putz, J. Regel, A. Wenzel and M. Bräunig, Thermal errors in milling: Comparison of displacements of the machine tool, tool and workpiece, *Procedia CIRP*, vol.82, pp.389-394, 2019.
- [13] H. Liu, E. M. Miao, X. D. Zhuang and X. Y. Wei, Thermal error robust modeling method for CNC machine tools based on a split unbiased estimation algorithm, *Precision Engineering*, vol.51, pp.169-175, 2018.
- [14] D. Dubrov, Cutting tool assembly with self-contained two-phase cooling system without hookup elements, *Materials Today: Proceedings*, vol.19, pp.2425-2428, 2019.
- [15] X. Thiem, B. Kauschinger and S. Ihlenfeldt, Structure model based correction of thermally induced motion errors of machine tools, *Procedia Manufacturing*, vol.14, pp.128-135, 2017.
- [16] J. Mayr, P. Blaser, A. Ryser and P. Hernandez-Becerro, An adaptive self-learning compensation approach for thermal errors on 5-axis machine tools handling an arbitrary set of sample rates, *CIRP Annals*, vol.67, no.1, pp.551-554, 2018.
- [17] C. Ma, J. Yang, L. Zhao and X. Mei, Simulation and experimental study on the thermally induced deformations of high-speed spindle system, *Appl. Thermal. Engr.*, vol.86, pp.251-268, 2015.
- [18] T. N. Reddy, V. Shanmugaraj, P. Vinod and S. G. Krishna, Real-time thermal error compensation strategy for precision machine tools, *Materials Today: Proceedings*, vol.22, pp.2386-2396, 2020.
- [19] M. Mareš, O. Horejš and L. Havlík, Thermal error compensation of a 5-axis machine tool using indigenous temperature sensors and CNC integrated Python code validated with a machined test piece, *Precision Engineering*, vol.66, pp.21-30, 2020.
- [20] F. C. Li, T. M. Li, Y. Jiang and H. Y. Wang, Explicit error modeling of dynamic thermal errors of heavy machine tool frames caused by ambient temperature fluctuations, *Journal of Manufacturing Processes*, vol.48, pp.320-338, 2018.
- [21] J. Y. Yan and J. G. Yang, Application of synthetic grey correlation theory on thermal point optimization for machine tool thermal error compensation, *The International Journal of Advanced Manufacturing Technology*, vol.43, pp.1124-1132, 2009.

- [22] Y. X. Li, J. G. Yang, T. Gelvis and Y. Y. Li, Optimization of measuring points for machine tool thermal error based on grey system theory, *The International Journal of Advanced Manufacturing Technology*, vol.35, pp.745-750, 2008.
- [23] *SINUMERIK 840D HMI Programming Package Part 1*, Chapter: 4-10, 2016.

### Author Biography



**Shuai Yang** received his Ph.D. of mechanical engineering from University of Ottawa, Canada in 2017. Now, he is an associate professor in Chongqing Technology and Business University. His research interests include vibration control, fault diagnosis and signal processing for mechanical system. From 2012 to now, he has published over 10 papers in his research field.



**Xing Luo** received her bachelor's degree of engineering management from Liaoning Technical University, China in 2019. Now, she is a graduate student of management science and engineering in Chongqing Technology and Business University. Her research interests include fault diagnosis and signal processing.



**Xu Chen** received her bachelor's degree from Dalian Ocean University in 2017. Now, she is a postgraduate in Chongqing Technology and Business University. Her research interests include fault diagnosis and signal processing.



**Zhiyong Luo** received his bachelor's degree from PLA Army Service Academy in 2009. Now, he is a engineer in Chongqing Banan District Quality Monitor Center of Road Engineering. His research interests include data analysis and mathematical model simulation.